

# Antenna Auto-Calibration and Metrology Approach for the AFRL/JPL Space Based Radar

Dalia McWatters, Adam Freedman, Thierry Michel and Vaughn Cable  
Jet Propulsion Laboratory, California Institute of Technology  
4800 Oak Grove Dr. Pasadena, CA 91109, USA

**Abstract-** The Air Force Research Laboratory (AFRL) and the Jet Propulsion Laboratory (JPL) are collaborating in the technology development for a space based radar (SBR) system that would feature a large aperture lightweight antenna for a joint mission later in this decade. This antenna system is a 50m x 2m electronically steerable phased array in L-band (1260 MHz center frequency, 80 MHz bandwidth) and contains 384 x 12 Transmit/Receive modules. The radar is designed to operate in a variety of modes including Synthetic Aperture Radar (SAR) and Moving Target Indication (MTI). Stringent requirements are placed on phase center knowledge and antenna sidelobe levels during a data take, in the presence of temperature changes due to the orbital thermal environment, self heating, spacecraft platform vibrations, and mechanical deformation. We present an auto-calibration and metrology system concept to correct for phase errors and mechanical deformation during the mission.

## I. INTRODUCTION

The Air Force Research Laboratory (AFRL) and the Jet Propulsion Laboratory (JPL) are collaborating in the technology development for a space based radar (SBR) system that would feature a large aperture lightweight antenna for a joint mission later in this decade. The orbit is 506 Km altitude.

The basic architecture of this radar system consists of a 50m x 2m electronically steerable phased array antenna in L band (1260 MHz, 80 MHz bandwidth). Scan range is  $\pm 45$  deg. in azimuth and  $\pm 20$  deg. in elevation. The array is composed of 32 panels (1.56m x 2m each). Each panel is composed of 12 x 12 radiating elements, each with its dedicated active Transmit/Receive (T/R) module. Each T/R module includes a power amplifier, low noise amplifier, circulator, phase shifter, programmable attenuator, polarization switch and calibration coupler and switches. The array can be commanded to transmit or receive in either H or V polarization. Each of the 32 panels has its own Panel Radar Electronics Module (PREM) where the RF network is combined (with appropriate true time delays), downconverted and digitized before being sent to the Digital Beam Former (DBF) by way of a fiber optic link. The PREM is also where the transmitted chirp and caltone signals are created and upconverted to L-band.

Fig. 1 shows a block diagram of the radar system. The radar is designed to operate in a variety of modes including Synthetic Aperture Radar (SAR) modes such as low resolution stripmap, high resolution stripmap and spotlight, as well as several Moving Target Indication (MTI) modes. The MTI modes, in particular, have a very stringent requirement

on phase center knowledge (a few millimeters) and antenna sidelobe level during receive (-50 dB rms).

During the mission, it is necessary to continuously measure the electrical phase of both the transmit and the receive paths associated with each radiating element, as well as the physical position of each radiating element with respect to a known reference point. This is due to the large size of the array, the stringent requirements on antenna flatness after compensation, the dynamics of the antenna structure, and the temperature gradients in the array due to self-heating of the electronics as well as non-uniform shading/illumination by the sun.

Various methods of calibrating phased array antennas were reported in the literature [1-6]. In [2], a continuous, on-board calibration system is presented, using a group of near-field sources emitting orthogonally coded calibration signals. This approach increases structural complexity for multiple calibration towers, requires an auxiliary calibration for the relative phase between sources and provides only the antenna receive path calibration. In [3], the full transmit array can be calibrated at once from space by encoding all the array elements with orthogonal complex gain and demodulating the conglomerate with a receiver on the ground. This method solves the low SNR/stability problem of calibrating each element individually but adds the complexity of orthogonal modulation and can't be done continuously throughout the orbit nor during data taking. Methods such as presented in [4] involve transmitting from one element while simultaneously receiving from its neighboring elements. However, this cannot be done during data taking and it does not resolve the transmit path separately from the receive path errors.

It became clear that a new method was needed, that would allow continuous calibration and metrology during data taking, and would resolve mechanical and transmit and receive phase errors without introducing prohibitive cost, mass and complexity.

## II. APPROACH

The physical position of each radiating element on the array is measured by the metrology system, using a set of cameras and triangulation techniques. The cameras are mounted on two calibration towers. The relative position between the towers is measured using laser ranging technology.

The RF calibration system measures the phase delay

associated with each antenna element electronics path, in both the transmit and the receive directions. The RF calibration system utilizes a calibration antenna/receiver on one of the towers, as well as electronics integrated into the antenna and radar electronic modules. Fig. 2 illustrates the calibration and metrology concept for the AFRL/JPL SBR antenna.

The calibration and metrology data are sent to the Calibration Processor, which computes in semi-real-time the necessary corrections in phase and time delay to each transmit/receive path. These corrections are communicated to the Radar Control Electronics, which translates and incorporates them into commands to the PREMs and the T/R modules. The correction is implemented using the same phase shifters and true time delays that control beam steering.

The metrology cameras are modified star-tracker cameras mounted in packs, in two positions above the center plane of the array. They continuously measure the physical position of targets on the radiating elements. The positions of the metrology packs are also measured relative to the radar coordinate reference. One of the metrology packs is mounted on the RF calibration tower. The tower is equipped with an omni-directional antenna and a receiver to route the RF calibration signals to the bus electronics for time delay and phase analysis by the calibration processor. Since the tower provides a common path for all the elements of the array, it provides the capability for making relative measurements.

In order to calibrate the relative delays in the transmit path, a sequence is conducted just prior to a data take, where each element transmitter is turned on, one at a time, and received by the calibration tower. The relative delays are corrected using panel analog true time delays, T/R module phase shifters, chirp generator timing and digitizer clock offsets. Since the sidelobe rejection requirements for transmit is not too stringent, we assume that a measurement prior to data taking (and after the array has sufficient warm up time) provides sufficient accuracy. If it is determined later that thermal changes of the radar electronics on the panel still contribute too much error during the data take, then it is possible to use thermal measurement data together with models generated in the laboratory prior to launch to improve the transmit phase estimate.

During the receive window, the requirement for phase knowledge is quite severe. Our plan is therefore to continuously inject calibration tones (generated by the Panel Radar Electronics Module) into each T/R module receive path in sequence. This calibration tone is embedded in the data and its phase delay and amplitude extracted in processing. Since the distribution of signals across the array has unknown phase delay characteristics over time, the injection phase of the caltone into each T/R module needs to be measured as well. By transmitting this caltone from each radiating element to the calibration tower, we can obtain this relative measurement across the array. In order to reduce the possibility of scan blindness when transmitting from a single element of the array to the tower, it is beneficial to electrically short the rest of the radiating elements to ground. This can be accomplished on the opposite polarization to the one currently used by the array, and is done by incorporating

a few additional switches to the T/R module front end.

### III. ANALYSIS AND SIMULATIONS

#### A. Description of analyses

In order to investigate the feasibility of this antenna metrology and calibration approach, several key analyses were required. First, it was necessary to show that it would be possible to transmit from each radiating element on the array to the cal tower without scan-blindness and in such a way that amplitude and phase response of this RF link can be predicted given the positions of the element and tower. This was achieved using electromagnetic simulations for the full field solution.

Second, a position was selected for the cal tower and the secondary metrology pack, such that the impact of these structures on the far-field pattern of the array was not significant and the metrology minimum baseline distance requirement was met.

In parallel with the above analyses, an antenna simulation model (ANTSIM) was constructed, which has the capability to accept inputs about the antenna physical deformation in addition to calibration and metrology errors. The simulation produces 3D antenna patterns and the calculated rms side-lobe level over the hemisphere.

In order to determine how often the metrology and calibration measurements have to be performed in the antenna array during the mission, several factors need to be considered. The spatial and temporal frequency of the metrology measurements are a function of the dynamics of the antenna structure. Using the Shuttle Radar Topography Mission (SRTM) experience, where an outboard antenna was mounted to the tip of a 60 m boom, it is reasonable to assume that a measurement rate of 1 to 10 Hz may be needed.

The RF calibration has to keep up with the phase and amplitude changes in the electronics that are primarily driven by temperature changes. Thermal analysis of the expected environment as well as analysis of phase vs. temperature of the calibration tone on SRTM was performed for this purpose. Results show that the antenna electronics may experience temperature changes of tens of degrees during orbit. Such a change will not progress uniformly over all the T/R modules and panel electronics. SRTM data indicates a rate of change of approximately 1 deg.phase/deg.C. Therefore, there could be very significant phase drifts in the radar electronics during a data take, which necessitates an autocalibration system that will remove these errors in real time.

#### B. ANTSIM results

ANTSIM models the components of the antenna, including the resolution of the phase shifters, programmable attenuators, and calibration and metrology errors. Antenna steering in azimuth and elevation can be applied as well as a mathematical description of the physical deformation of the radiating surface. Fig. 3 shows the azimuth cut of the antenna pattern in the presence of antenna deformation when no correction is made, compared with correcting for this

deformation using nominal system errors. The following nominal errors were determined to have a negligible effect on the antenna performance: metrology position errors of 2mm in xyz, rotational errors of 0.1 deg., calibration phase errors of 2 deg. calibration gain errors of 0.5 deg. and timing errors of 1ps. The deformation used was a quadratic with 20 cm deflection at each end of the 50m length, superimposed with a quadratic deformation of each mechanical panel, of 3cm rms deflection. No compensation leads to about 3 dB degradation in the rms sidelobe level over the hemisphere and 45% broadening of the main lobe. This level of degradation significantly violates performance requirements.

### C. Element to tower link analysis

An antenna model was constructed for the full field solution, using method of moments. Patch radiating elements were constructed on a ground plane, with the appropriate spacing, radiating one at a time to a pickup probe antenna at the correct position on the tower. The probe picked up both polarizations and the amplitude and phase of the link were computed. To bring computation time to a reasonable duration, the array was modeled as a ground plane except for a row of 24x1 patches that was slid through the array. Only the center three elements of this row were excited, one at a time, before the row was slid forward by 3 patch positions. The result of one of these simulations is shown in Fig. 4. Simulations of this type suggest that the link was well behaved (i.e. had no scan-blindness or excessive dynamic range) from various element positions to the tower.

Fig. 5 shows the result of a comparison between two simulations of the 24x1 row (sliding by steps of 3), where the tower probe position had been offset by 4 cm compared with the nominal position. The amplitude change is less than 1 dB and the phase change is well behaved. This result indicates that it should be possible to correct for the tower motion (which would be measured by the metrology system) in semi-real-time and still meet the calibration accuracy requirements.

### D. Effect of towers on far field

In order to determine the effect of the towers on the far field antenna pattern, it was necessary to simulate the full array by using dipoles, since patch elements made the computations prohibitively long. The dipole and the patch differ in their radiation pattern primarily at small angles relative to the aperture plane. These shallow angles would apply to the interactions in the near-field related to the tower structures. Therefore, although the far field pattern is fairly accurate, the effect of the tower(s) in this type of simulation is only a first order estimate of the degree to which the physical presence of the towers/metrology packs affect the far field radiating pattern of the antenna array.

Fig. 6 shows the results of a simulation where the two metrology packs, represented by 10x10x10cm conductive cubes, were placed at 6m baseline separation along the center of the 50m length of the antenna, and 2 m above the antenna plane. There is no significant difference between the far field patterns in the elevation or azimuth cut, nor the side

lobe level statistics with or without the towers. The same results are true for a 4m baseline.

## IV. METROLOGY

Several factors governed the design of the metrology system: 1) Since the antenna is long and the thermal environment not benign, antenna and panel distortions should be directly measurable without relying on theoretical modeling. 2) Hundreds or thousands of locations on the antenna surface need to be tracked so that simple interpolation can yield element phase center locations to the required accuracy level. 3) This constellation of targets must be measured at a high update rate (several Hz or better), as some mechanical oscillation modes are close to 1 Hz and thermal deformation effects can be rapid if, for example, the antenna plunges from full sunlight into eclipse. 4) A minimum number of metrology hardware platforms should be employed, as their relative positions must also be measured to a very high accuracy. 5) The metrology system should employ hardware that currently exists (a technology "cutoff" of 2005), with only modifications of software or firmware. 6) Element phase centers should be measured to approximately the 2 mm level in all three dimensions, although the measurement in-and-out of the antenna plane is somewhat more important than the in-plane deformation, both because it is the more probable deformation and it affects the beam pattern more.

A single metrology platform would require metrology units that could determine the 3-D positions of large numbers of targets with a high update rate. This technology is not yet available, although scanning lidar and similar 3-D measurement technology is under development to make this solution more feasible in several years. Rather, a two-platform metrology solution was chosen, with each tower-mounted platform containing a set of cameras that image each antenna target (Fig. 2 and Fig. 7). Thus, the position of each target may be determined by stereo viewing using simple photogrammetric triangulation techniques. Two platforms also allow one platform to be used to define an antenna reference coordinate system tied to inertial space, while the position and attitude of the second platform can easily be measured with respect to the first.

A simple geometric triangulation model indicated that the cameras could do their job if they were located approximately 2 m above the antenna plane and at least 6 m apart. The height above the plane was required to distinguish individual targets at the far end of the antenna 25 m away and to see them if the antenna bowed "down", away from the cameras, up to 10 cm (the current estimated maximum possible deformation). The minimum distance between the cameras, the measurement "baseline", is governed by the cameras' resolution of the most distant targets and the required "along-plane" (x-axis) position accuracy required for those targets. The baseline length chosen, 6 m, is adequate for reasonable focal length cameras imaging the ends of the antenna, although along-plane positions may not be determined to the full 2 mm accuracy. ANTSIM analysis indicated that random

end-of-antenna along-plane uncertainties of 4 mm would have negligible impact on the resultant beam characteristics.

Two candidate imaging hardware solutions were identified. Both allow for small imaging units on the towers creating as little blockage of, or interference with, the main antenna RF beam pattern as possible. Both are low power, low mass units to minimize mass and structural complexity of the towers (a significant cost driver for the metrology/calibration system). One uses CCD (charge-coupled device) technology, an older and more proven technology for space applications [7]. The other uses CMOS (complementary metal oxide semiconductor) "camera-on-a-chip" technology, a technology that is newer but has several advantages over CCD imagers such as smaller size, better radiation performance and longevity, and less bleeding and better rejection of sun-glint and direct sun [8]. Careful shielding and filtering may be required to protect the imaging electronics from the radiating antenna, for either imaging solution.

Both passive and active target constellations on the antenna panel were considered. A passive target scheme might consist of a set of omnidirectional reflective targets similar to those used in terrestrial laser distance measurements, illuminated by flash units on the calibration towers. The flash units would trigger in rapid sequence and the imagers would detect the locations of the individual reflectors.

We prefer an active target system, however, consisting of a constellation of illuminated LEDs. This solution allows more flexibility, as the LEDs may be pulsed or colored differently to distinguish close targets, and there is no reliance on a single unit, such as a flash unit, whose failure would result in many targets being lost. Moreover, distant target LEDs could be made brighter or more tightly aimed. An active LED array has to be integrated much more closely with the panel electronics and structural components, and could have a more significant effect on the RF antenna properties than would a passive system. We are currently considering placing the LED at the center of the radiating patch element, where it should have minimal effect on the antenna pattern.

One platform, located on the metrology tower, would also contain a global positioning system (GPS) receiver and a star tracker to determine the absolute position and orientation of that platform. This platform would provide the primary antenna reference frame for the radar. The other platform, on the calibration tower, would contain a laser ranging and/or camera system sufficient to determine the position and orientation of the calibration platform relative to the metrology platform at the sub-millimeter level (Fig. 7).

To achieve sub-pixel resolution, defocusing of the target image to fill a 3x3 pixel imaging area is required. LED targets must be spaced far enough apart so that they can be reliably distinguished from their neighbors and their defocused images do not corrupt the centroid computation of the neighboring targets. This is more of a challenge given the great depth of field required for most of the imaging optics, and could potentially require specially shaped lensing

systems. Preliminary analyses indicate that none of these issues should be significant in practice, and that the LEDs could be strobed in patterns such that the visual separation between illuminated targets increases. Bright artifacts due to specular reflections should also not be a problem, as "LED off" images can be subtracted from "LED on" images. Current commercial LEDs are bright enough and provide more than enough SNR even at the 25 m maximum viewing distance.

We have performed some simple simulations using MATLAB<sup>®</sup> to assess how many cameras might be needed and their required fields of view, focal lengths and  $f/\#$ s. We require that individual LED targets, which are mounted on alternate antenna elements, have at least an 8-10-pixel target-to-target spacing to avoid centroid aliasing. We also use the simulation to verify that 2 m tall towers can image the entire deformed antenna surface without any target obscuration, and to estimate what the actual recovered target position accuracies would be.

Based on the simulations, a set of 14 cameras, seven on each tower, provides an excellent metrology system for our needs. Three cameras on each tower face forward, three face aft, and one faces the center of the antenna. It is quite possible, however, that fewer cameras might be needed once the design is optimized.

The simulation and camera study indicates that camera focal lengths between 6.5 mm (central camera) and 75 mm (end camera) are needed, with  $f/\#$ s between 1.3 and 6.3, respectively. These values are reasonable for small camera optics, although the end cameras will weigh quite a bit more than the others due to their longer focal lengths and larger lenses (e.g. 100 gm vs. 10 gm for CMOS imagers).

The recovered position accuracy is shown in Fig. 8. Note that the along-plane (x-axis) error is a factor of two or more larger than the other two components, especially towards the ends of the antenna. The overall RMS error is under 0.4 mm. Although the total error increases towards the ends of the antenna and at the edges of the camera fields, rarely does it exceed 1 mm. This configuration allows all the element locations to be determined to better than a 2 mm level in each dimension, as required. Also, all targets remain in view even with cubic deformation along the antenna reaching 10 cm at the two ends.

## V. SUMMARY

We developed a concept for an autocalibration and metrology system for a 50m x 2m electronically steerable array that would meet the requirements without posing an unreasonable burden on mission resources in terms of cost, mass, power, and complexity. The analysis tools are now in place and further optimization and refinements are ready to be done as the mission definition progresses.

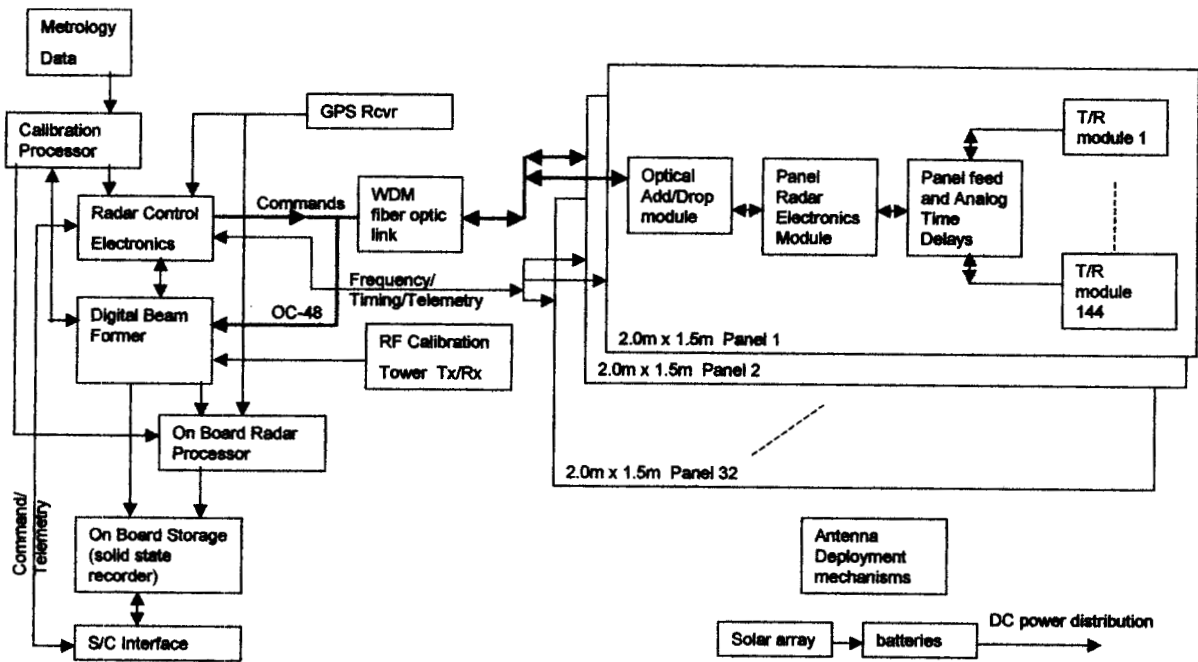


Figure 1: Block diagram of the AFRL/JPL radar instrument

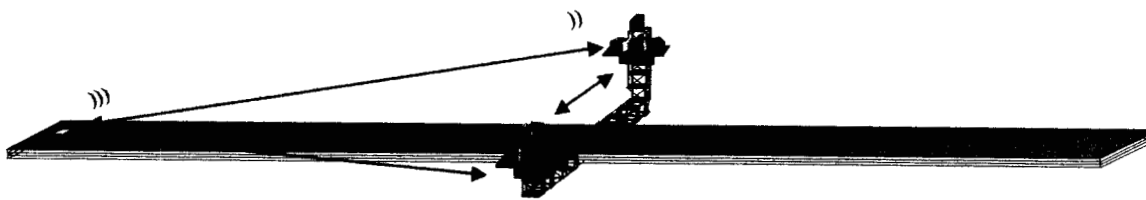


Figure 2: AFRL/JPL SBR metrology and calibration concept

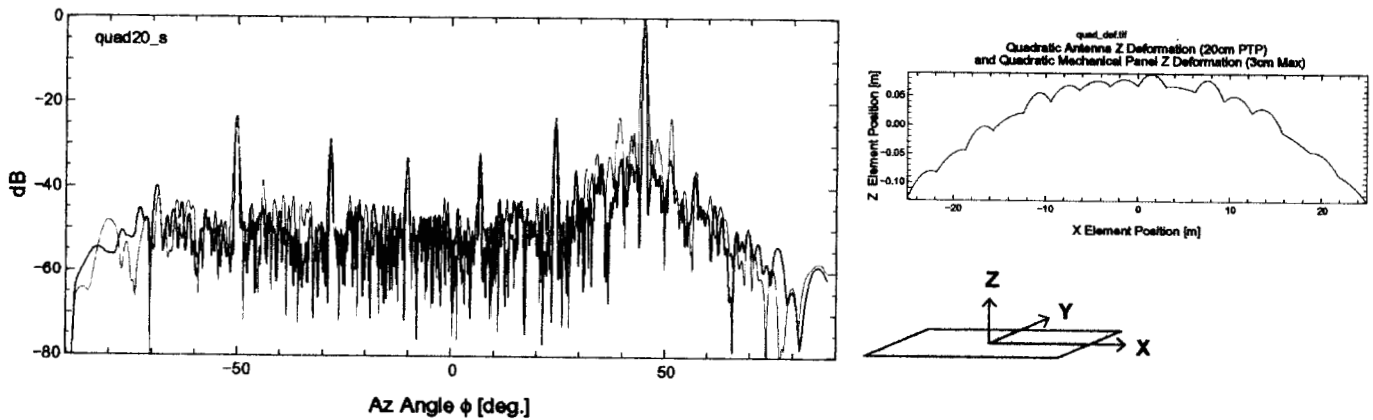


Figure 3: ANTSIM result showing effect of antenna deformation

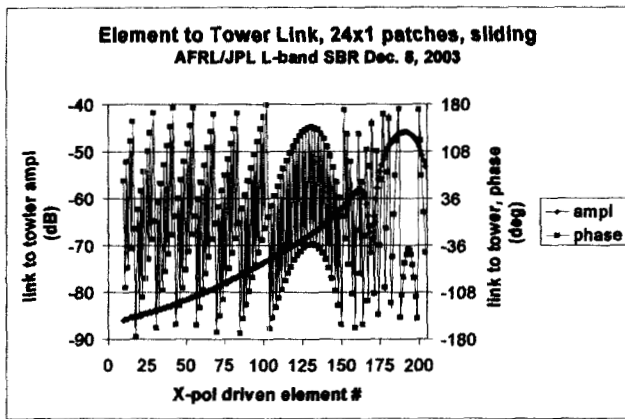


Figure 4: Element to tower link, near field simulation

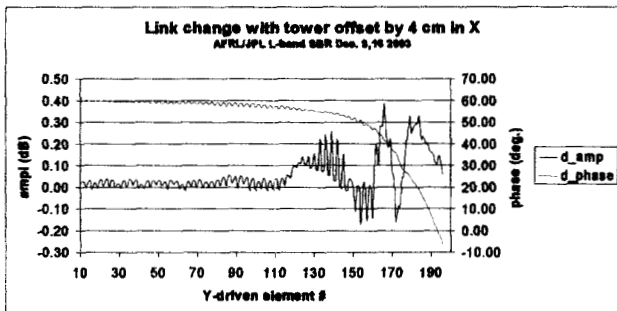
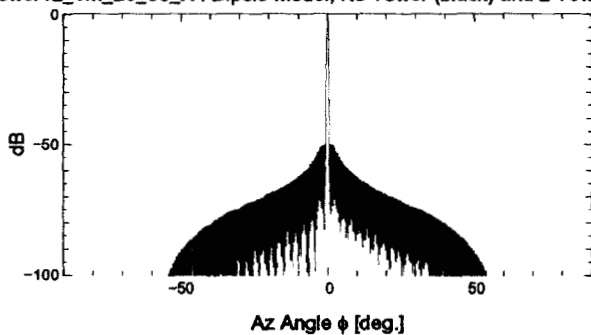


Figure 5: Element to tower link, change with tower motion

Azimuth Array Factor, steering: [0,20] deg, BW offset: 0 MHz  
Tower12\_6m\_20\_90\_X : Dipole Model, No Tower (black) and 2 Towers (red)



(parFile)Name="db020.rtf", AZSteerAngle=0.010916, AZSteerIPRW=0.365995, AZSteerIPRW=1.16895, AZSteerIPRW=06.7088, AZSteerIPRW=50.1988, ElSteerAngle=10.9367, ElSteerIPRW=7.82654, ElSteerIPRW=20.4095, ElSteerIPRW=-18.4797, ElSteerIPRW=-5.76249, FullSideLobePeak=-5.76249, FullSideLobeRMS=-25.7315)

(parFile)Name="db020.rtf", AZSteerAngle=0.010916, AZSteerIPRW=0.366146, AZSteerIPRW=1.16895, AZSteerIPRW=06.7106, AZSteerIPRW=50.1523, ElSteerAngle=19.5387, ElSteerIPRW=7.82855, ElSteerIPRW=20.4095, ElSteerIPRW=-18.4799, ElSteerIPRW=-5.76251, FullSideLobePeak=-5.76251, FullSideLobeRMS=-43.7315)

Elevation Antenna Factor

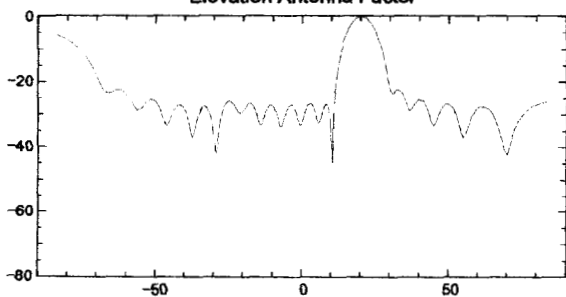


Figure 6: Far field pattern, two metrology packs, 6m baseline, vs. no towers

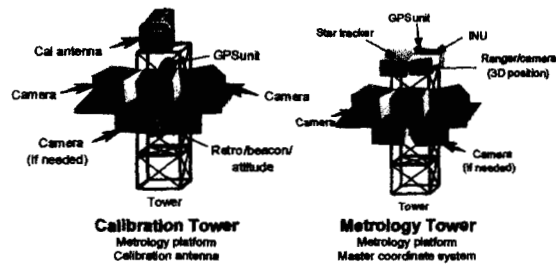


Figure 7. Conceptual illustration of the two metrology towers and platforms.

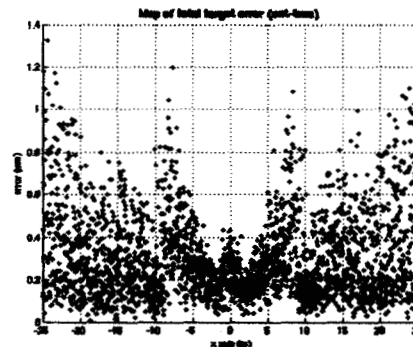


Figure 8. Estimated target position errors from the simulation. The x axis lies along the 50m length of the antenna, with total 3D RSS error shown along the vertical axis.

#### ACKNOWLEDGMENT

The work described in this paper was carried out at the Jet Propulsion Laboratory, California Institute of Technology under a contract with the National Aeronautics Space Agency. Our thanks to Eric Gurrola and Francois Rogez of JPL for processing the SRTM temperature and caltone phase data. We thank Patrick Wu and Shonte Wright of JPL for thermal simulation data. Our thanks also to Bedabrata Pain of JPL for the Advanced CMOS Sensor analysis.

#### REFERENCES

- [1] J.J. Schuss, J. Upton, B. Myers, T. Sikina, A. Rohwer, P. Makridakas, R. Francois, L. Wardle, W. Kreutel and R. Smith, "The Iridium main mission antenna concept," *IEEE AES Systems Magazine*, 0885-8985, vol. 12, pp. 3-12, Dec. 1997.
- [2] W. Yao, Y. Wang and T. Itoh, "A Self-calibration antenna array system with moving apertures," *IEEE MTT-S International Microwave Symposium Digest*, v 3, 2003, pp. 1541-1544
- [3] S.D. Silverstein, "Remote calibration of active phased array antennas for communication satellites," *Acoustics, Speech, and Signal Processing, ICASSP-97, IEEE International Conference on*, Volume: 5, 21-24 April 1997 pp.4057 - 4060
- [4] C. Shipley and D. Woods, "Mutual coupling-based calibration of phased array antennas," *Phased Array Systems and Technology*, 2000. Proceedings, *IEEE International Conference on*, 21-25 May 2000 pp.529 - 532.
- [5] E. Lee and C. N. Dorny, "A Broadcast reference technique for self-calibrating of large antenna phased arrays," *IEEE Transactions on Antennas and Propagation*. vol. 37. no.8 , pp. 1003-1010, August 1989
- [6] R.X. Meyer, "Electronic compensation for structural deformations of large space antennas," *Astrodynamics Proceedings of the Conference*, Vail, CO, August 12- 15, 1985. Part 1 (A86-43201 20-12). San Diego, CA, Univelt, Inc., 1986, p. 277-285.
- [7] J.L. Jorgensen, C.C. Liege, "The advanced stellar compass, development and operations," *Acta Astronautica*, Vol. 39 (9-12), pp. 775-783, Nov.-Dec. 1996[server4.oersted.dtu.dk/research/ASC/index].
- [8] R. Nixon, et. al "256X256 CMOS active pixel sensor camera-on-a-ip," *IEEE J. Solid-State Circuits*, Vol. 31 (12), pp. 2046-2050, Dec. 1996. [aps.jpl.nasa.gov/integratedaps/index.html].